

Pro-cathepsin D interacts with the extracellular domain of the {beta} chain of LRP1 and promotes LRP1-dependent fibroblast outgrowth

Mélanie Beaujouin ¹, Christine Prébois ¹, Danielle Derocq ¹, Valérie Laurent-Matha ¹, Olivier Masson ¹, Sophie Pattingre ¹, Peter Coopman ², Nadir Bettache ², Jami Grossfield ³, Robert E. Hollingsworth ³, Hongyu Zhang ⁴, Zemin Yao ⁴, Bradley T. Hyman ⁵, Peter Van Der Geer ⁶, Gary K. Smith ⁷, Emmanuelle Liaudet-Coopman ^{1*}

¹ IRCM, Institut de recherche en cancérologie de Montpellier INSERM : U896 , Université Montpellier I , CRLC Val d'Aurelle - Paul Lamarque F-34298 Montpellier,FR

² CRBM, Centre de recherches de biochimie macromoléculaire CNRS : UMR5237 , Université Montpellier I , Université Montpellier II - Sciences et Techniques du Languedoc , IFR122 , 1919 Route de Mende 34293 MONTPELLIER CEDEX 5,FR

³ Genetics Research GlaxoSmithKline , Inc. Five Moore Drive, Research Triangle Park, North Carolina, 27709,US

⁴ Department of Biochemistry, Microbiology and Immunology University of Ottawa , Ottawa K1Y4W7,CA

⁵ Alzheimer Disease Research Laboratory Harvard Medical School , Massachusetts General Hospital , Charlestown, Massachusetts 02129,US

⁶ Department of Chemistry and Biochemistry San Diego State University , 5500 Campanile Drive, MC 1030, San Diego, CA 92182-1030,US

⁷ Screening and Compound Profiling GlaxoSmithKline , Inc. Five Moore Drive, Research Triangle Park, North Carolina, 27709,US

* Correspondence should be addressed to: Emmanuelle Liaudet-Coopman <emmanuellemmanuelle.liaudet-coopman@inserm.fr >

Abstract

SUMMARY

Interactions between cancer cells and fibroblasts are crucial in cancer progression. We have previously shown that the aspartic protease cathepsin-D (cath-D), a marker of poor prognosis in breast cancer that is overexpressed and highly secreted by breast cancer cells, triggers mouse embryonic fibroblast outgrowth via a paracrine loop. Here, we show the requirement of secreted cath-D for human mammary fibroblast outgrowth using a three-dimensional coculture assay with breast cancer cells that do or do not secrete pro-cath-D. Interestingly, proteolytically-inactive pro-cath-D remains mitogenic, indicating a mechanism involving protein-protein interaction. We identify the LDL receptor-related protein-1, LRP1, as a novel binding partner for pro-cath-D in fibroblasts. Pro-cath-D binds to residues 349-394 of the β chain of LRP1, and is the first ligand of the extra-cellular domain of LRP1 β to be identified. We show that pro-cath-D interacts with LRP1 β in cellulo . Interaction occurs at the cell surface, and overexpressed LRP1 β directs pro-cath-D to the lipid rafts. Our results reveal that the ability of secreted pro-cath-D to promote human mammary fibroblast outgrowth depends on LRP1 expression, suggesting that pro-cath-D/LRP1 β interaction plays a functional role in the outgrowth of fibroblasts. Overall, our findings strongly suggest that pro-cath-D secreted by epithelial cancer cells promotes fibroblast outgrowth in a paracrine LRP1-dependent manner in the breast tumor micro-environment.

Author Keywords cathepsin D ; LRP1 ; tumor micro-environment ; cancer ; fibroblast outgrowth

INTRODUCTION

Tumor progression has been recognized as the product of evolving cross-talk between tumor cells and the surrounding supportive tissue, known as the tumor stroma (Mueller and Fusenig, 2004). Cancer cells interact dynamically with several normal cell types within the extracellular matrix, such as fibroblasts, infiltrating immune cells, endothelial cells and adipocytes, (Mueller and Fusenig, 2004). Stromal and tumor cells exchange enzymes, growth factors and cytokines that modify the local extracellular matrix, stimulate migration and invasion, and promote the proliferation and survival of stromal and tumor cells (Liotta and Kohn, 2001 ; Masson et al., 1998).

The aspartic protease cathepsin D (cath-D) is overexpressed and highly secreted by human epithelial breast cancer cells (Capony et al., 1989 ; Liaudet-Coopman et al., 2006 ; Rochefort and Liaudet-Coopman, 1999 ; Vignon et al., 1986). Its overexpression in breast cancer is correlated with poor prognosis (Ferrandina et al., 1997 ; Foekens et al., 1999 ; Rodriguez et al., 2005). Human cath-D is synthesized as a 52-kDa precursor that is rapidly converted in the endosomes to form an active, 48-kDa, single-chain intermediate, and then in the lysosomes into the fully active mature protease, composed of a 34-kDa heavy chain and a 14-kDa light chain. The human cath-D catalytic site includes two critical aspartic residues (amino acids 33 and 231) located on the 14-kDa and 34-kDa chains, respectively (Metcalf and Fusek, 1993). The overexpression of cath-D in breast cancer cells leads to the hypersecretion of the 52-kDa pro-cath-D into the extracellular environment (Heylen et al., 2002 ; Laurent-Matha et al., 1998 ; Vignon et al., 1986). Secreted pro-cath-D can be endocytosed by both cancer cells and fibroblasts (Heylen et al., 2002 ; Laurent-Matha et al., 1998 ; Vignon et al., 1986), mainly via the mannose-6-phosphate receptors (M6PR), or by alternative cath-D receptors (Capony et al., 1994 ; Laurent-Matha et al., 2005 ; Rijnboutt et al., 1991). Cath-D affects both cancer cells and stromal cells in the tumor microenvironment by increasing cancer cell proliferation,

metastasis, angiogenesis and the three-dimensional growth (outgrowth) of fibroblasts embedded in a Matrigel matrix (Berchem et al., 2002 ; Glondu et al., 2001 ; Glondu et al., 2002 ; Hu et al., 2008 ; Laurent-Matha et al., 2005 ; Vignon et al., 1986). We had previously observed that a mutated catalytically-inactive version of cath-D (D231N) remains mitogenic for tumor cells and mouse embryonic fibroblasts (Berchem et al., 2002 ; Glondu et al., 2001 ; Laurent-Matha et al., 2005), suggesting that cath-D may act as an extracellular messenger that interacts either directly or indirectly with an as-yet unidentified cell surface receptor.

In the present study, we show that pro-cath-D hypersecreted by cancer cells stimulates the outgrowth of human mammary fibroblasts embedded in a Matrigel matrix, thus indicating for the first time the relevance of the paracrine role of secreted cath-D in a pathological context. We also identify the LDL receptor-related protein-1 (LRP1) as a novel binding partner for cath-D in fibroblasts, and present data in support of a functional role for this interaction in the outgrowth of fibroblasts induced by epithelial cancer cells. LRP1 is composed of a 515-kDa extracellular α chain, and an 85-kDa β chain (Lillis et al., 2005 ; Strickland and Ranganathan, 2003). The extracellular α chain contains binding-sites for many structurally unrelated ligands, including lipoprotein particles, proteases and protease-inhibitor complexes. The β chain contains an extracellular domain, a trans-membrane region, and a cytoplasmic tail. At present, the ligands of the extracellular domain of the LRP1 β chain are still unknown. In this study, we report for the first time the interaction between pro-cath-D and the extracellular domain of the β chain of LRP1.

RESULTS

Pro-cath-D secreted by cancer cells stimulates 3D outgrowth of human mammary fibroblasts

The communication between epithelial cancer cells and fibroblasts plays a crucial role in cancer progression. We had previously developed a three-dimensional (3D) co-culture system showing that human breast cancer MCF-7 cells induce outgrowth of mouse embryonic, human skin, and breast fibroblasts, indicating that these epithelial cancer cells secrete paracrine factors capable of promoting fibroblast outgrowth in 3D matrices (Laurent-Matha et al., 2005). These factors included cath-D, and we demonstrated that secreted cath-D was involved in the outgrowth of mouse embryonic cath-D-deficient fibroblasts independently of its catalytic activity (Laurent-Matha et al., 2005).

In order to study the relevance of the paracrine role of secreted pro-cath-D in the context of human breast cancer, we have now performed our 3D co-culture system using human mammary fibroblasts (HMF) (Fig. 1A , panel a). To find out whether secreted pro-cath-D might be one of the crucial paracrine factors affecting HMF outgrowth, 3D co-culture assays were carried out using MCF-7 cells (Fig. 1A , panel c) in which endogenous pro-cath-D secretion was reduced by 75% by small RNA-mediated gene silencing (cath-D siRNA) for 2 days before the co-culture assay (Fig. 1A , panel d). MCF-7 cells transfected with cath-D siRNA (Fig. 1A , panel b, middle) were less effective in triggering HMF fibroblast outgrowth than MCF-7 cells transfected with control luciferase siRNA (luc siRNA) (Fig. 1A , panel b, left). 75% inhibition of pro-cath-D secretion by cath-D siRNA still occurred during our co-culture assay, even after 3 days of co-culture (Fig. 1A , panel d). In contrast, in HMF fibroblasts embedded alone (Fig. 1A , panel b, right), pro-cath-D secretion was not detected after 3 days of co-culture (Fig. 1A , panel d). We conclude that the inhibition of pro-cath-D secretion in breast cancer cells rapidly reduces human mammary fibroblast outgrowth.

To analyze the role of the catalytic activity of secreted pro-cath-D, we then carried out 3D co-culture assays with cath-D-transfected rat 3Y1-Ad12 cancer cell lines secreting either no human cath-D (control), or hyper-secreting either human wild-type cath-D (cath-D) or D231N mutated cath-D devoid of proteolytic activity (D231N) (Fig. 1B , panel b). Only the 3Y1-Ad12 cancer cells secreting wild-type or D231N pro-cath-D (Fig. 1B , panel c) stimulated HMF fibroblast outgrowth, and the 3Y1-Ad12 control cells had no effect (Fig. 1B , panel a), suggesting that secreted catalytically-inactive pro-cath-D promotes 3D outgrowth of human mammary fibroblasts in a paracrine manner. Overall, our findings support the concept that pro-cath-D secreted by epithelial cancer cells may display a crucial paracrine effect on breast fibroblasts in a manner independent of its catalytic activity.

Cath-D interacts with the LRP1 receptor in vitro

Since cath-D hypersecreted by cancer cells is able to stimulate fibroblast outgrowth in a paracrine manner which is independent of its catalytic activity, we postulate that pro-cath-D secreted by cancer cells may act via its interaction with potential receptors present on the fibroblast cell surface. To identify possible cath-D partners, we performed a yeast two-hybrid screen using a LexA DNA-binding domain fused to 48-kDa intermediate cath-D as bait, and a cDNA library isolated from normal breast. The clone isolated in our screen was 100% identical to amino acids 307-479 of the extracellular domain of the LRP1 β chain (Fig. 2A).

To validate the cath-D/LRP1 interaction, we next performed GST pull-down experiments. The polypeptide containing amino acids 307-479 of the extracellular domain of the LRP1 β chain, GST-LRP1 β (307-479), was expressed as a GST fusion protein, and tested for its ability to bind to pro-cath-D (Fig. 2B , left panel). Our results show that pro-cath-D bound to GST-LRP1 β (307-479) (Fig. 2B , right panel). Subsequently, we performed GST pull-down experiments using GST-fusion proteins containing the 52-kDa pro-cath-D, 34-kDa cath-D

heavy chain, 14-kDa cath-D light chain, or 4-kDa cath-D propeptide (Fig. 2C , left panels). The full-length extracellular LRP1 β domain, LRP1 β (1-476), was shown to bind effectively to 52-, 34- and 14-kDa cath-D fragments, but poorly to 4-kDa cath-D propeptide (Fig. 2C , right panels), indicating that the interaction interface spans both the 34- and 14-kDa cath-D sub-units.

The LRP1 β (307-479) domain contains four juxtaposed complete EGF-like repeats (19-22) (Fig. 3A , panel a). In order to identify the LRP1 β cath-D-binding domain, GST-fusion proteins containing various fragments of LRP1 β (307-479) were tested for their ability to bind to pro-cath-D (Fig. 3A , panel b). We identified the F4 fragment of LRP1 β (349-394) that contains the EGF-like repeat 20, as the shortest fragment able to bind pro-cath-D, when compared to F7 (307-348), F6 (394-432) or F8 (433-479) fragments of LRP1 β (Fig. 3B , panel a). It is worth noting that LRP1 β (307-479) also contains other important domains, since the F4(349-394) fragment was partially active in pro-cath-D binding when compared to F0(307-479). The abilities of smaller LRP1 β fragments (F5, F9-F13) derived from F4, and of the F14 fragment covering the entire EGF-like repeat 20 (residues 360-396) to interact with pro-cath-D (Fig. 3B , top and bottom panels a and b) were both significantly impaired, suggesting that the intact F4(349-394) fragment is required for the cath-D/LRP1 β interaction. Because of the lack of disulfide linkage in *E. coli* , we verified that binding of pro-cath-D was comparable after GST-LRP1 β F0 and F4 refolding (Fig. 3B , panel c). Our results provide independent confirmation of the yeast two-hybrid screen, and reveal direct interaction between cath-D and residues 349-394 of the extracellular domain of the LRP1 β chain.

Pro-cath-D partially co-localizes with LRP1 at the cell surface in transfected COS cells and in fibroblasts

We next investigated whether pro-cath-D colocalizes with LRP1 β at the cell surface of intact cells. Non-permeabilized COS cells transiently co-transfected with pro-cath-D and Myc-LRP1 β were analyzed by immunocytochemistry after double staining with a monoclonal antibody recognizing only the pro-cath-D proform, and a polyclonal antibody directed against the N-terminal Myc-tag of LRP1 β . Figure 4A shows that pro-cath-D (in red; panel b) partially co-localized (panel c) with LRP1 β (in green; panel a) in punctuate structures. To confirm that secreted pro-cath-D colocalizes with LRP1 at the cell surface, cellular co-localization of LRP1 and pro-cath-D was further analyzed by immunogold electron microscopy in COS cells transiently co-transfected with pro-cath-D and LRP1 β after double staining with an anti-pro-cath-D monoclonal antibody and a polyclonal antibody directed against the cytoplasmic tail of LRP1 β (Fig. 4B). We observed co-localization of pro-cath-D and the LRP1 β chain at the cell surface (Fig. 4B). Co-localization at the cell surface was also observed in COS cells transiently transfected with LRP1 β and incubated with 15-nM pro-cath-D (data not shown). To investigate the interaction of secreted cath-D with endogenous LRP1, HMF fibroblasts were incubated with 15 nM of pro-cath-D, and co-localization was analyzed by immunogold electron microscopy (Fig. 4C). Our data reveal that in HMF fibroblasts pro-cath-D and LRP1 β co-localize at the cell surface (Fig. 4C). Altogether, our findings indicate that, in intact cells, pro-cath-D and LRP1 β co-localize at the cell surface.

Overexpressed LRP1 β directs pro-cath-D to lipid rafts in transfected COS cells

Previous report described that LRP1 is localized both at the cell surface and in early endosomes (Herz and Strickland, 2001). Interestingly, some of the cell surface LRP1 is located in lipid rafts (Wu and Gonias, 2005 ; Zhang et al., 2004). Therefore, we next investigated whether pro-cath-D and LRP1 might be co-located at the cell surface in these micro-domains. COS cells transfected with cath-D (Fig. 5 , panel a) or co-transfected with pro-cath-D and LRP1 β (Fig. 5 , panel b) were subjected to sucrose density ultracentrifugation. The raft markers, flotillin and ganglioside GM1, were found predominantly in the low density fractions 4–6, whereas the non-raft marker, transferrin receptor (TfR), was found at the bottom of the sucrose gradient (Fig. 5 , bottom panels). Endogenous LRP1 β was detected in both the raft-rich and non-raft fractions (Fig. 5 , panel a, top). Pro-cath-D was mainly located in the non-raft fractions 7 and 8, although both pro-cath-D and its 48-kDa intermediate form were also detected in the raft-rich fractions 5 and 6 (Fig. 5 , panel a, middle). Interestingly, overexpression of LRP1 β (Fig. 5 , panel b, top) resulted in a significant increase of pro-cath-D in the raft-rich fractions (Fig. 5 , panel b, middle). These findings reveal, for the first time, the presence of pro-cath-D at the cell surface in lipid rafts, and strongly suggest that LRP1 β enrichment in lipid rafts can direct pro-cath-D to these micro-domains.

Cath-D interacts with LRP1 β in transfected COS cells and in fibroblasts

To find out whether pro-cath-D interacts with the LRP1 β chain in cellulo , LRP1 β was co-transfected into COS cells in the presence of wild-type pro-cath-D or of a pro-cath-D mutant devoid of proteolytic activity (^{D231N} cath-D). Unfortunately, no antibody recognizing only pro-cath-D was available for immunoprecipitation. We therefore used the anti-cath-D MIG8 antibody that recognizes the 52-, 48-, and 34-kDa forms of cath-D. This meant that immunoprecipitation with MIG8 would precipitate extracellular 52-kDa pro-cath-D associated with the cell surface, and intracellular 52-, 48- and 34-kDa forms of cath-D. Our results using anti-LRP1 β antibody show that wild-type and D231N pro-cath-D were both co-immunoprecipitated with LRP1 β (Fig. 6A , panel a, top). Longer gel exposure revealed that mature 34-kDa cath-D was also coimmunoprecipitated with LRP1 β (Fig. 6A , panel b), suggesting that pro-cath-D and the associated LRP1 β chain can be directed to the lysosomes. Reciprocally, LRP1 β was co-immunoprecipitated with cath-D or ^{D231N} cath-D using anti-cath-D MIG8 antibody (Fig. 6A , panel a, bottom). ^{D231N} cath-D displayed greater electrophoretic mobility, corresponding to an apparent molecular mass shift of ~1 kDa (Fig. 6A , panel a, top), as previously reported (Laurent-Matha et al., 2006). These findings demonstrate that the LRP1 β chain interacts preferentially with the 52-kDa pro-cath-D. We therefore conclude that co-transfected pro-cath-D and LRP1 β interact in cellulo .

In order to study endogenous interaction in intact cells, we screened a variety of cell lines for LRP1 expression (Fig. S1). Cath-D is known to be overexpressed and hypersecreted by breast cancer cells (Capony et al., 1989), but our survey revealed that breast cancer cells (MCF-7 and MDA-MB-231) express low levels of LRP1 (Fig. S1). In contrast, LRP1 was highly expressed in all the fibroblastic cell lines tested: PEA10 (LRP1^{+/+} MEF), CD55^{-/-}-cath-D (cath-D^{-/-} MEF transfected with human cath-D), and CCL146 mouse fibroblasts, HMF and CCD45K human fibroblasts (Fig. S1). However, as previously reported, fibroblasts do not secrete detectable levels of pro-cath-D (Laurent-Matha et al., 2005).

Since the cells that express high LRP1 levels and those that secrete pro-cath-D are distinct, we next studied the interaction of cath-D with endogenous LRP1 β using cath-D^{-/-} MEF cells stably transfected with human wild-type (CD55^{-/-}-cath-D) or mutated D231N cath-D (CD55^{-/-}-D231N) that had previously been shown to hypersecrete pro-cath-D (Laurent-Matha et al., 2005). Anti-cath-D M1G8 immunoaffinity purification revealed that LRP1 β was co-eluted with both wild-type (Fig. 6B, panel a) and D231N cath-D (Fig. S2). These results indicate that endogenous LRP1 interacts with stably transfected cath-D in fibroblasts.

We finally investigated the interaction of cath-D with endogenous LRP1 β in HMF fibroblasts incubated with 15 nM of pro-cath-D by immunoaffinity purification using M1G8 antibody. LRP1 β was co-eluted with cath-D (Fig. 6B, panel b). We conclude that endogenous LRP1 β interacts with cath-D in fibroblasts. Altogether, our data indicate that pro-cath-D interacts with LRP1 β in cellulo.

Human cath-D requires LRP1 expression to trigger 3D outgrowth of fibroblasts

As we had identified LRP1 as the novel fibroblastic receptor for pro-cath-D, we went on to check whether cath-D would induce fibroblast outgrowth via its interaction with LRP1.

To investigate the possible implication of LRP1 in the cath-D-induced fibroblast outgrowth, we performed 3D culture assays in cath-D transfected-fibroblasts hyper-secreting pro-cath-D (CD55^{-/-}-cath-D) or mutated D231N pro-cath-D (CD55^{-/-}-D231N), which had or had not been silenced for LRP1 (Fig. 7A, panel a). As previously shown (Laurent-Matha et al., 2005), cath-D^{-/-} MEF cells transfected with an empty vector (CD55^{-/-}-SV40) did not grow in Matrigel, and transfecting wild-type or mutated cath-D into cath-D^{-/-} MEF cells led to a switch to fibroblast outgrowth (Fig. 7A, panel b), indicating cath-D-induced fibroblast outgrowth. We therefore analyzed the consequences of silencing LRP1 in these cells. The effect of LRP1 silencing on CD55^{-/-}-cath-D outgrowth was shown by phase-contrast microscopy (Fig. 7B, panel a, top), and by cell staining (Fig. 7B, panel a, bottom). Our findings indicate that LRP1 silencing in CD55^{-/-}-cath-D cells using LRP1 siRNA3 (Fig. 7B, panel c) significantly reduced their cath-D-dependent outgrowth compared to cells transfected with Luc siRNA (Fig. 7B, panels a and b). Similar results were observed using LRP1 siRNA4 (Fig. S3). These findings indicate that cath-D requires LRP1 expression to promote fibroblast outgrowth. However, interestingly, LRP1 silencing in CD55^{-/-}-D231N cells also significantly inhibited their outgrowth, indicating the existence of a mechanism independent of cath-D proteolytic activity (Fig. 7C).

To further investigate whether LRP1 mediates the paracrine action of secreted pro-cath-D on fibroblast outgrowth, we next performed 3D co-culture assays (Fig. 8, panel a) with Luc- or LRP1-silenced HMFs (Fig. 8, panel b), co-cultured with 3Y1-Ad12 cancer cells secreting or not secreting wild-type or D231N cath-D (Fig. 8, panel c). The co-culture assay revealed that only pro-cath-D-secreting 3Y1-Ad12 cells stimulated the outgrowth of HMF fibroblasts transfected with Luc siRNA, in contrast to 3Y1-Ad12 control cells (Fig. 8, panel d). This outgrowth was shown by phase-contrast microscopy (Fig. 8, panel d, top), and by cell staining (Fig. 8, panel d, bottom). Our results further showed that silencing LRP1 in HMF fibroblasts using siRNA1 (Fig. 8, panel e) blocked their mitogenic response to secreted pro-cath-D as shown by phase-contrast microscopy (Fig. 8, panel e, top), and by cell staining (Fig. 8, panel e, bottom). Similar results were obtained with LRP1 siRNA2 (Fig. S4). In control experiments, we confirmed that the viability of HMF cells remained unaffected by LRP1-silencing. Phase-contrast microscopy showed that HMFs transfected with Luc siRNA adopted an elongated morphology typical of fibroblasts (Fig. S5, panels a and b (see insets)). LRP1 silencing using siRNA1 or siRNA2 analyzed by western blot (Fig. S5, panels a and b) induced a rounder shape and fewer protrusions when compared to Luc siRNA-transfected cells (Fig. S5, panels a and b (see insets)). This suggests that LRP1 expression is required for the elongated fibroblast 3D morphology. The cell viability of HMF cells embedded in Matrigel was, however, not altered by LRP1-silencing. This was shown by cell staining in Matrigel (Fig. S5, panel a, bottom), and by cell cycle analyses using flow cytometry of cells extracted from Matrigel (S+G2M = 17% for Luc siRNA HMF cells; S+G2M = 19.7% for LRP1 siRNA1 HMF cells). Altogether, these findings highlight that pro-cath-D secreted by epithelial cancer cells promotes fibroblast outgrowth in a paracrine, LRP1-dependent manner (Fig. 9).

DISCUSSION

In this report, we identify the LRP1 receptor as a novel binding partner for pro-cath-D in fibroblasts. The cath-D/LRP1 β interaction discovered by a yeast two-hybrid screen was further confirmed by GST pull-down, co-immunoprecipitation, co-purification and co-localization. Our results demonstrate that, in fibroblasts, the pro-cath-D protease interacts with the extracellular domain of the β chain of LRP1, and establishes pro-cath-D as the first ligand of the extracellular LRP1 β chain to be identified. We identified the F4 LRP1 β (349-394) fragment, that contains the EGF-like repeat 20 with an additional 11 amino acids at its N-terminus, as the shortest fragment able

to bind pro-cath-D. No ligand has previously been described as binding to this particular region, and the biological relevance of the EGF-like repeats in the extracellular domain of LRP1 β is still unknown. Our results reveal that pro-cath-D colocalized with LRP1 β at the cell surface in lipid rafts. At the cell surface, LRP1 has been shown to be localized in clathrin-coated pits and in lipid rafts (Boucher et al., 2002 ; Wu and Gonias, 2005 ; Zhang et al., 2004). Here, we show that LRP1 β overexpression directs pro-cath-D to the lipid rafts. Interestingly, this study reveals, for the first time, the presence of pro-cath-D in lipid rafts. The lysosomal cysteine protease cath-B is also known to localize within these lipid micro-domains in association with the annexin II heterotetramer (Mohamed and Sloane, 2006). A previous study excluded LRP1 as a possible cath-D receptor (Laurent-Matha et al., 2002). These observations were based on the use of the RAP chaperone protein (Herz, 2006), which competes with ligands that bind to the LRP1 α chain (Laurent-Matha et al., 2002). We checked that RAP protein did not bind to LRP1 β , and that the pro-cath-D/LRP1 β interaction was not abolished by RAP (data not shown). Consequently, our finding that cath-D binds to the LRP1 β chain explains why RAP did not compete with cath-D for binding to LRP1.

Cancer is a tissue-based disease in which malignant cells interact dynamically with many normal cell types, such as fibroblasts (Mueller and Fusenig, 2004). The fibroblast is a major cell type of the stromal compartment, and is intimately involved in orchestrating the stromal part of the dialogue in tissue homeostasis (Grinnell, 1994 ; Elenbaas et al., 2001). A stromal reaction immediately adjacent to transformed epithelial cells has been documented in several tumor systems (Basset et al., 1990). Whereas the role of matrix metalloproteinases and urokinase plasminogen activator in the stromal compartment has been documented in various studies (Liotta and Kohn, 2001), the potential role of cath-D in fibroblasts has not yet been fully determined. It has been proposed that cath-D localized at the surface of breast fibroblasts might be mitogenic (Koblinski et al., 2002), or that intracellular cath-D in fibroblasts might assist cancer cells to digest the extracellular matrix during tissue invasion (Heylen et al., 2002). We had previously observed that pro-cath-D secreted by cancer cells mediates mouse embryonic fibroblast outgrowth in a paracrine manner (Laurent-Matha et al., 2005), suggesting its key role in the tumor microenvironment. In the present study, we validate these findings in human mammary fibroblasts, indicating the relevance of the paracrine role of secreted pro-cath-D in the tumor microenvironment in the pathological context. We also demonstrate that LRP1 is the fibroblastic receptor responsible for stimulating the pro-cath-D-induced outgrowth. Our 3D co-culture outgrowth assays with cancer cells, which did or did not secrete human pro-cath-D, and human mammary fibroblasts, which had or had not been silenced for LRP1, reveal that pro-cath-D requires LRP1 expression to promote human mammary fibroblast outgrowth. These data support a model in which pro-cath-D hypersecreted by cancer cells stimulates the outgrowth of surrounding fibroblasts in a paracrine and LRP1-dependent manner in the breast tumor-microenvironment. It is worth noting that LRP1 may be involved in the onset and progression of various human malignancies, since LRP1 is expressed by fibroblasts in breast cancer biopsies, and also at the invasive front in colon cancer biopsies (Christensen et al., 1996 ; Obermeyer et al., 2007). In addition, C766T LRP1 gene polymorphism is associated with an increased risk of breast cancer development (Benes et al., 2003). Moreover, recent studies have reported a stimulatory role of LRP1 in cancer cell proliferation, motility and invasion (Dedieu et al., 2008 ; Li et al., 2003 ; Song et al., 2009). Although breast cancer cells express LRP1 at a much lower level than fibroblasts, several studies have reported that hypoxia significantly up-regulates LRP1 expression in breast cancer cells (Bando et al., 2003 ; Koong et al., 2000 ; Montel et al., 2007). It is therefore possible that cath-D-enhanced breast cancer cell proliferation may be also dependent on LRP1 expression, acting via an autocrine loop. Our outgrowth assays using cells hyper-secreting pro-cath-D or not, and silenced for LRP1 or not, strongly suggest that cath-D may also promote outgrowth via LRP1 in an autocrine manner. Future studies will investigate the possible relevance of the autocrine function of cath-D via LRP1 in breast cancer cells.

The mechanism by which LRP1 controls the cath-D-dependent stimulation of fibroblast outgrowth implies that cath-D has an action independent of its catalytic activity. The serine protease tPA has also been shown to act independently of its proteolytic activity as a cytokine via LRP1 (Hu et al., 2006). LRP1 is known to modify the extracellular micro-environment by internalizing numerous ligands via its α -chain (Herz and Strickland, 2001), to control signal transduction pathways via cytoplasmic LRP1 β tyrosine phosphorylation (Barnes et al., 2003 ; Boucher and Gotthardt, 2004 ; Boucher et al., 2002 ; Hu et al., 2006 ; Yang et al., 2004), and to modulate gene transcription by Regulated Intramembrane Proteolysis (RIP) of its β chain (Kinoshita et al., 2003 ; May et al., 2002 ; von Arnim et al., 2005 ; Zurhove et al., 2008). Future research will investigate whether the pro-cath-D/LRP1 β complex is internalized, and whether the pro-cath-D/LRP1 β interaction can affect LRP1 β tyrosine phosphorylation or LRP1 β RIP.

In conclusion, we report, for the first time, that pro-cath-D interacts with the extracellular domain of LRP1 β chain at the surface of fibroblasts, and that it promotes a LRP1-dependent fibroblast outgrowth independently of its catalytic activity. We propose that pro-cath-D, which is hypersecreted by breast cancer cells, may be involved in creating the tumor micro-environment that can sustain breast tumor growth and progression through its interaction with LRP1.

MATERIALS AND METHODS

Materials

Human mammary fibroblasts (HMFs), kindly provided by J. Piette (IGM, Montpellier, France), were obtained from reduction mammoplasty tissues from a patient without cancer. Cath-D-deficient CD55 $^{-/-}$ immortalized mouse fibroblasts transfected with empty vector (CD55 $^{-/-}$ -SV40), human cath-D (CD55 $^{-/-}$ -cath-D), and D231N mutated cath-D (CD55 $^{-/-}$ -D231N) were previously described (Laurent-Matha et al., 2005). 3Y1-Ad12 rat cancer cells transfected with empty vector (3Y1-Ad12/control), human cath-D

(3Y1-Ad12/cath-D), or D231N mutated cath-D (3Y1-Ad12/D231N) were previously described (Glondou et al., 2001). PEA13 (^{LRP1}-/- MEF) and PEA10 (^{LRP1}+/- MEF) were purchased from ATCC. Cells were cultured in DMEM medium with 10% fetal calf serum (FCS, GibcoBRL). The 11H4 hybridoma directed against the C-terminal intracellular part of LRP1 β chain was purchased from ATCC. Polyclonal anti-human LRP1 β -chain antiserum directed against the C-terminal intracellular part of LRP1 β chain was previously described (Zhang et al., 2004). The anti-human, cath-D monoclonal antibody M2E8, used for immuno-fluorescence, interacts only with 52-kDa pro-cath-D, and not with 48- or 34-kDa cath-D (Freiss et al., 1988). The anti-human cath-D monoclonal antibody (BD Biosciences) used for immunoblotting recognized 52-, 48- and 34-kDa forms of cath-D. The anti-human cath-D MIG8 monoclonal antibody used for immunoprecipitation and immunoaffinity purification recognized 52-, 48- and 34-kDa forms of cath-D (Garcia et al., 1985). Control IgG1 MOPC-21 monoclonal antibody was purchased from Abcam, anti- β actin polyclonal antibody from Sigma, anti-human Flotillin-1 monoclonal antibody from BD Biosciences, and anti-human Transferrin receptor monoclonal antibody from Zymed. Pro-cath-D content of culture supernatants was determined by using a cath-D immunoradiometric assay (Garcia et al., 1985).

Plasmids

pcDNA3.1(+)*Myc*-tagged LRP1 β chain (Barnes et al., 2003), pcDNA3.1(-)cath-D, and pcDNA3.1(-)^{D231N} cath-D expression plasmids (Glondou et al., 2001) have previously been described (Glondou et al., 2001). The pcDNA3.1(+)*LRP1* β extracellular domain (1-476) expression plasmid was created by inserting the PCR-amplified cDNA encoding LRP1 β (1-476) from pcDNA3.1(+)*Myc*-tagged LRP1 β into pcDNA3.1(+) previously digested by *Nhe* I and *Xba* I. pGEX-4T-1 LRP1 β (307-479) was generated by inserting PCR-amplified cDNA encoding LRP1 β (307-479) from pYESTrp2-*LRP1* β (307-479) identified by a two-yeast hybrid assay into pGEX-4T-1 previously digested by *Eco* RI. GEX-4T-1 LRP1 β smaller fragments were generated by inserting PCR-amplified cDNA LRP1 β shorter fragments from pYESTrp2-*LRP1* β (307-479) into pGEX-4T-1 previously digested by *Eco* RI and *Xho*I. Supplemental Table 1 shows the primers used for LRP1 β cloning. pGEX-2TK-cath-D constructs were obtained by inserting PCR-amplified cDNA encoding human 52 kDa pro-cath-D, 34 kDa and 14 kDa cath-D chains, and 4 kDa cath-D pro-fragment into pGEX-4T-1 previously digested by *Eco* RI. Supplemental Table 1 shows the primers used for cath-D cloning.

Yeast two-hybrid assay

Human cath-D (48 kDa intermediate form) was fused with the LexA DNA-binding domain in the pMW101 vector. A cDNA library derived from normal breast tissue was cloned into the galactosidase-inducible pYESTrp2 vector (Invitrogen) containing a B42 activating domain. The yeast two-hybrid screen was performed as described previously (Slentz-Kesler et al., 2000).

siRNA transfections and outgrowth assays

30,000 HMF cells were transiently transfected with 10- μ g human LRP1 or Luc siRNAs using Oligofectamine (Invitrogen). 50,000 CD55^{-/-}-cath-D or CD55^{-/-}-D231N cells were transiently transfected with 2.5 μ g mouse LRP1 or Luc siRNAs. 15,000 MCF-7 cells were transiently transfected with 1 μ g siRNA using Oligofectamine (Invitrogen). For outgrowth assays, 50,000 CD55^{-/-}-cath-D or CD55^{-/-}-D231N cells were re-suspended at 4°C in Matrigel (BD Biosciences) 24 h post-transfection with LRP or Luc siRNAs, and added to a pre-set layer of Matrigel (Glondou et al., 2001). In co-culture outgrowth assays, 15,000 MCF-7 cells previously transfected with cath-D or luc siRNAs, or 100,000 cells from control-, D231N-, or cath-D-transfected 3Y1-Ad12 cell lines were plated and then covered first with a layer of Matrigel, and then with a layer of Matrigel containing 50,000 HMFs 48-h post-transfection with LRP or Luc siRNAs (Laurent-Matha et al., 2005).

siRNAs

Duplexes of 21-nucleotide human LRP1 siRNA1 (target sequence AAGCAGTTTGCCTGCAGAGAT, residues 666-684) (Li et al., 2003), human LRP1 siRNA2 (target sequence AAGCTATGAGTTTAAGAAGTT) (Dharmacon), mouse LRP1 siRNA3 (target sequence AAGCAUCUCAGUAGACUAUCA) (Fears et al., 2005), mouse LRP1 siRNA4 (target sequence AAGCAGTTTGCCTGCAGAGAC), human cath-D siRNA (target sequence AAGCUGGUGGACCAGAACAUC, residues 666-684) (Bidere et al., 2003), or firefly luciferase (Luc) siRNA (target sequence AACGTACGCGGAATACTTCGA) were synthesized by MWG Biotech S.A. (France) or Dharmacon. Supplemental Table 1 shows siRNA oligonucleotides.

GST pull-down assays

[³⁵S]methionine-labeled pre-pro-cath-D, and LRP1 β (1-476) were obtained by transcription and translation using the TNT^{T7}-coupled reticulocyte lysate system (Promega). GST, GST-*LRP1* β fragments, and GST-cath-D fusion proteins were produced in *Escherichia coli* B strain BL21 using isopropyl-1-thio- β -D-galactopyranoside (1 mM) for 3 h at 37°C. GST fusion proteins were purified on glutathione-Sepharose beads (Amersham Biosciences). For pull-down assays, 20- μ l of glutathione-Sepharose beads with immobilized GST fusion proteins were incubated overnight at 4°C with [³⁵S]methionine-labeled proteins in 500 μ l PDB buffer (20 mM HEPES-KOH [pH 7.9], 10% glycerol, 100 mM KCl, 5 mM MgCl₂, 0.2 mM EDTA, 1 mM DTT, 0.2 mM phenylmethylsulfonyl fluoride) containing 15 mg/ml BSA and 0.1% Tween 20. The beads were washed with 500 μ l PDB buffer, and bound proteins were resolved by 15% SDS-PAGE, stained

with Coomassie blue, and exposed to autoradiographic film. The refolding of GST proteins was performed using a multi-step dialysis protocol (Protein refolding kit, Novagen) followed by disulfide bond formation using a redox system (cysteine/cystine).

Co-transfection, co-immunoprecipitation and co-purification

COS cells were co-transfected with 10 µg of pcDNA3-Myc-LRP1β, and 10 µg of pcDNA3.1, pcDNA3.1-cath-D or pcDNA3.1-D231N cath-D vectors. Transient transfection was carried out using Lipofectamine and Opti-MEM (Gibco-BRL). Two days post-transfection, cells were directly lysed in 50 mM Hepes [pH 7.5], 150 mM NaCl, 10% glycerol, 1% Triton X-100, 1.5 mM MgCl₂, 1 mM EGTA, 100 mM NaF, 10 mM sodium pyrophosphate, 500 µM sodium vanadate, and a protease inhibitor cocktail (PLC lysis buffer). Lysates were incubated with 3 µg of anti-cath-D M1G8, or control IgG1 MOPC-21 monoclonal antibodies, or 40 µl of the anti-LRP1β 11H4 hybridoma overnight at 4°C, and subsequently with 25 µl of 10% protein G-Sepharose, for 2 h at 4°C on a shaker. Sepharose beads were washed 4 times with PLC buffer, boiled for 3 min in SDS sample buffer, and resolved by SDS-PAGE and immunoblotting. For cath-D purification, unwashed cells were lysed in PLC buffer and were passed over an anti-cath-D M1G8-coupled agarose column. The column was washed with phosphate buffer (0.5 M NaPO₄, 150 mM NaCl, 0.01% Tween 80, 5 mM β-glycerophosphate) containing protease inhibitors, and then eluted in different fractions with 20 mM lysine, pH 11.

Isolation of lipid rafts

COS cells transfected as described above were lysed in MEB buffer (150 mM NaCl, 20 mM Morpholine Ethane Sulfonic acid, [pH 6.5]) containing 1% Triton X100, 1 mM Na₃VO₄, 50 mM NaF, and protease inhibitor cocktail, and were homogenized using a Dounce homogenizer. The preparation was mixed with an equal volume of 80% sucrose solution in MEB buffer in an ultracentrifuge tube over-laid with 30% sucrose and 1.5 ml of 5% sucrose, and centrifuged at 39,000 rpm for 16 h at 4°C in a Beckman SW40 Ti. After centrifuging, fractions were collected and subjected to immunoblot analysis. The ganglioside GM1 was detected with biotin-conjugated cholera toxin B subunit (Sigma-Aldrich) followed by incubation with horseradish peroxidase-conjugated streptavidin and revealed by chemiluminescence (ECL, GE Healthcare).

Immunoblotting

Cell extracts (100 µg) or conditioned media (80 µl) were submitted to SDS-PAGE and anti-LRP1β, anti-cath-D, or anti-βactin immuno-blotting.

Immunocytochemistry

Cells co-transfected with pro-cath-D and Myc-LRP1β were fixed with 4% paraformaldehyde and blocked with 2.5% goat serum (Sigma). Cells were incubated with the A-14 rabbit polyclonal antibody (10 µg/ml, Santa Cruz) recognizing the 9E10 Myc tag followed by an AlexaFluor 488-conjugated goat anti-rabbit IgG (1/200; Invitrogen). After washing, cells were incubated with an anti-pro-cath-D M2E8 mouse monoclonal (40 µg/ml) followed by an AlexaFluor 568-conjugated goat anti-mouse IgG (1/200; Invitrogen). DNA was visualized by incubation with 0.5 µg/ml cell-permeant Hoechst 33342 dye (Molecular Probes; 10 min). Microscopy slides were observed with a motorized Leica Microsystems (Rueil-Malmaison, France) DMRA2 microscope equipped with an oil immersion x100/1.4 apochromatic objective and a 12-bit Coolsnap FX CCD camera (Princeton Instruments, Roper Scientific, Evry, France), both controlled by the MetaMorph imaging software (Universal Imaging, Roper Scientific).

Immunogold

Cells grown in 24-well inserts were fixed with 3% paraformaldehyde and 0.1% glutaraldehyde in a phosphate buffer [pH 7.2] overnight at 4°C. Cells were cryoprotected with sucrose 3.5 %, stained for 2 h with uranyl acetate 2% in a maleate buffer 0.05 M [pH 6.2] at room temperature. Cells were embedded in Lowicryl HM20 in a Leica EM AFS using the Progressive Lowering of Temperature method. Ultra-thin sections (85 nm) were first pre-incubated in PBS with 0.1% cold water fish gelatin, 1% BSA, and 0.05% Tween 20 (incubation buffer) for 2 h at room temperature, and then incubated with rabbit anti-LRP1β (1/20) and mouse anti-cath-D M2E8 (40 µg/ml) in the incubation buffer overnight at 4°C, and subsequently with 15 nm goat anti-rabbit-gold and 6 nm goat anti-mouse-gold 5 (Aurion) diluted 1/20 in the incubation buffer for 2 h at 4°C. Sections were observed under a Hitachi 7100 transmission electron microscope.

Flow cytometry

Cells embedded in Matrigel were recovered after 3 days with 2.5 ml Matrisperse (Becton Dickinson), re-suspended in 1 ml of a solution containing 0.1% tri-sodium citrate dehydrate, 0.1% Triton X-100, 25 µg/ml propidium iodide and 100 µg/ml RNase, prior to FACScan analysis (Becton Dickinson, CA) with an argon ion laser turned at 488nm, 20 mW. Propidium iodide fluorescence was measured at 585 nm. Data were collected and analyzed with Cellquest (Becton Dickinson, CA) and ModFit (Verity Software, ME) software, respectively.

Acknowledgements:

We would like to thank Nadia Kerdjadj for secretarial assistance, Jean-Yves Cance for the photographs, and Chantal Cazevielle (Centre de Ressources en Imagerie Cellulaire, Montpellier) for the immunogold microscopy. We would also thank Stephan Jalaguier for helpful discussions regarding the GST pull-down experiments. This work was supported by the 'Institut National de la Santé et de la Recherche Médicale', University of Montpellier I, 'ANR Jeunes Chercheuses, Jeunes Chercheurs' and the 'Ligue Nationale contre le Cancer', and the 'Association pour la Recherche sur le Cancer', which provided a fellowship for Mélanie Beaujoui.

References:

- Bando H, Toi M, Kitada K, Koike M. 2003; Genes commonly upregulated by hypoxia in human breast cancer cells MCF-7 and MDA-MB-231. *Biomed Pharmacother.* 57 : 333 - 40
- Barnes H, Ackermann EJ, van der Geer P. 2003; v-Src induces Shc binding to tyrosine 63 in the cytoplasmic domain of the LDL receptor-related protein 1. *Oncogene.* 22 : 3589 - 97
- Basset P, Bellocq JP, Wolf C, Stoll I, Hutin P, Limacher JM, Podhajcer OL, Chenard MP, Rio MC, Chambon P. 1990; A novel metalloproteinase gene specifically expressed in stromal cells of breast carcinomas. *Nature.* 348 : 699 - 704
- Benes P, Jurajda M, Zaloudik J, Izakovicova-Holla L, Vacha J. 2003; C766T low-density lipoprotein receptor-related protein 1 (LRP1) gene polymorphism and susceptibility to breast cancer. *Breast Cancer Res.* 5 : R77 - 81
- Berchem G, Glondu M, Gleizes M, Brouillet JP, Vignon F, Garcia M, Liaudet-Coopman E. 2002; Cathepsin-D affects multiple tumor progression steps in vivo: proliferation, angiogenesis and apoptosis. *Oncogene.* 21 : 5951 - 5
- Bidere N, Lorenzo HK, Carmona S, Laforge M, Harper F, Dumont C, Senik A. 2003; Cathepsin D triggers Bax activation, resulting in selective apoptosis-inducing factor (AIF) relocation in T lymphocytes entering the early commitment phase to apoptosis. *J Biol Chem.* 278 : 31401 - 11
- Boucher P, Gotthardt M. 2004; LRP and PDGF signaling: a pathway to atherosclerosis. *Trends Cardiovasc Med.* 14 : 55 - 60
- Boucher P, Liu P, Gotthardt M, Hiesberger T, Anderson RG, Herz J. 2002; Platelet-derived growth factor mediates tyrosine phosphorylation of the cytoplasmic domain of the low density lipoprotein receptor-related protein in caveolae. *J Biol Chem.* 277 : 15507 - 13
- Capony F, Braulke T, Rougeot C, Roux S, Montcourrier P, Rochefort H. 1994; Specific mannose-6-phosphate receptor-independent sorting of pro-cathepsin D in breast cancer cells. *Exp Cell Res.* 215 : 154 - 63
- Capony F, Rougeot C, Montcourrier P, Cavailles V, Salazar G, Rochefort H. 1989; Increased secretion, altered processing, and glycosylation of pro-cathepsin D in human mammary cancer cells. *Cancer Res.* 49 : 3904 - 9
- Christensen L, Wiborg Simonsen AC, Heegaard CW, Moestrup SK, Andersen JA, Andreasen PA. 1996; Immunohistochemical localization of urokinase-type plasminogen activator, type-I plasminogen-activator inhibitor, urokinase receptor and alpha(2)-macroglobulin receptor in human breast carcinomas. *Int J Cancer.* 66 : 441 - 52
- Dedieu S, Langlois B, Devy J, Sid B, Henriot P, Sartelet H, Bellon G, Emonard H, Martiny L. 2008; LRP-1 silencing prevents malignant cell invasion despite increased pericellular proteolytic activities. *Mol Cell Biol.* 28 : 2980 - 95
- Elenbaas B, Spirio L, Koerner F, Fleming MD, Zimonjic DB, Donaher JL, Popescu NC, Hahn WC, Weinberg RA. 2001; Human breast cancer cells generated by oncogenic transformation of primary mammary epithelial cells. *Genes Dev.* 15 : 50 - 65
- Fears CY, Grammer JR, Stewart JE Jr, Annis DS, Mosher DF, Bornstein P, Gladson CL. 2005; Low-density lipoprotein receptor-related protein contributes to the antiangiogenic activity of thrombospondin-2 in a murine glioma model. *Cancer Res.* 65 : 9338 - 46
- Ferrandina G, Scambia G, Bardelli F, Benedetti Panici P, Mancuso S, Messori A. 1997; Relationship between cathepsin-D content and disease-free survival in node-negative breast cancer patients: a meta-analysis. *Br J Cancer.* 76 : 661 - 6
- Foekens JA, Dall P, Klijn JG, Kroch-Angel P, Claassen CJ, Look MP, Ponta H, Van Putten WL, Herrlich P, Henzen-Logmans SC. 1999; Prognostic value of CD44 variant expression in primary breast cancer. *Int J Cancer.* 84 : 209 - 15
- Freiss G, Vignon F, Rochefort H. 1988; Characterization and properties of two monoclonal antibodies specific for the Mr 52,000 precursor of cathepsin D in human breast cancer cells. *Cancer Res.* 48 : 3709 - 15
- Garcia M, Capony F, Derocq D, Simon D, Pau B, Rochefort H. 1985; Characterization of monoclonal antibodies to the estrogen-regulated Mr 52,000 glycoprotein and their use in MCF7 cells. *Cancer Res.* 45 : 709 - 16
- Glondu M, Coopman P, Laurent-Matha V, Garcia M, Rochefort H, Liaudet-Coopman E. 2001; A mutated cathepsin-D devoid of its catalytic activity stimulates the growth of cancer cells. *Oncogene.* 20 : 6920 - 9
- Glondu M, Liaudet-Coopman E, Derocq D, Platet N, Rochefort H, Garcia M. 2002; Down-regulation of cathepsin-D expression by antisense gene transfer inhibits tumor growth and experimental lung metastasis of human breast cancer cells. *Oncogene.* 21 : 5127 - 34
- Grinnell F. 1994; Fibroblasts, myofibroblasts, and wound contraction. *J Cell Biol.* 124 : 401 - 4
- Herz J. 2006; The switch on the RAPP's necklace. *Mol Cell.* 23 : 451 - 5
- Herz J, Strickland DK. 2001; LRP: a multifunctional scavenger and signaling receptor. *J Clin Invest.* 108 : 779 - 84
- Heylen N, Vincent LM, Devos V, Dubois V, Remacle C, Trouet A. 2002; Fibroblasts capture cathepsin D secreted by breast cancer cells: possible role in the regulation of the invasive process. *Int J Oncol.* 20 : 761 - 7
- Hu K, Yang J, Tanaka S, Gonias SL, Mars WM, Liu Y. 2006; Tissue-type plasminogen activator acts as a cytokine that triggers intracellular signal transduction and induces matrix metalloproteinase-9 gene expression. *J Biol Chem.* 281 : 2120 - 7
- Hu L, Roth JM, Brooks P, Luty J, Karparkin S. 2008; Thrombin up-regulates cathepsin D which enhances angiogenesis, growth, and metastasis. *Cancer Res.* 68 : 4666 - 73
- Kinoshita A, Shah T, Tangredi MM, Strickland DK, Hyman BT. 2003; The intracellular domain of the low density lipoprotein receptor-related protein modulates transactivation mediated by amyloid precursor protein and Fe65. *J Biol Chem.* 278 : 41182 - 8
- Koblinski JE, Dosesco J, Samen M, Moin K, Clark K, Sloane BF. 2002; Interaction of human breast fibroblasts with collagen I increases secretion of procathepsin B. *J Biol Chem.* 277 : 32220 - 7
- Koong AC, Denko NC, Hudson KM, Schindler C, Swiersz L, Koch C, Evans S, Ibrahim H, Le QT, Terris DJ. 2000; Candidate genes for the hypoxic tumor phenotype. *Cancer Res.* 60 : 883 - 7
- Laurent-Matha V, Derocq D, Prebois C, Katunuma N, Liaudet-Coopman E. 2006; Processing of human cathepsin D is independent of its catalytic function and auto-activation: involvement of cathepsins L and B. *J Biochem.* 139 : 363 - 71
- Laurent-Matha V, Farnoud MR, Lucas A, Rougeot C, Garcia M, Rochefort H. 1998; Endocytosis of pro-cathepsin D into breast cancer cells is mostly independent of mannose-6-phosphate receptors. *J Cell Sci.* 111 : (Pt 17) 2539 - 49
- Laurent-Matha V, Lucas A, Huttler S, Sandhoff K, Garcia M, Rochefort H. 2002; Procathepsin D interacts with prosaposin in cancer cells but its internalization is not mediated by LDL receptor-related protein. *Exp Cell Res.* 277 : 210 - 9
- Laurent-Matha V, Maruani-Herrmann S, Prebois C, Beaujoui M, Glondu M, Noel A, Alvarez-Gonzalez ML, Blacher S, Coopman P, Baghdiguian S. 2005; Catalytically inactive human cathepsin D triggers fibroblast invasive growth. *J Cell Biol.* 168 : 489 - 99
- Li Y, Lu W, Bu G. 2003; Essential role of the low density lipoprotein receptor-related protein in vascular smooth muscle cell migration. *FEBS Lett.* 555 : 346 - 50
- Liaudet-Coopman E, Beaujoui M, Derocq D, Garcia M, Glondu-Lassis M, Laurent-Matha V, Prebois C, Rochefort H, Vignon F. 2006; Cathepsin D: newly discovered functions of a long-standing aspartic protease in cancer and apoptosis. *Cancer Lett.* 237 : 167 - 79
- Lillis AP, Mikhailenko I, Strickland DK. 2005; Beyond endocytosis: LRP function in cell migration, proliferation and vascular permeability. *J Thromb Haemost.* 3 : 1884 - 93

- Liotta LA , Kohn EC . 2001 ; The microenvironment of the tumour-host interface . *Nature* . 411 : 375 - 9
- Masson R , Lefebvre O , Noel A , Fahime ME , Chenard MP , Wendling C , Kebers F , LeMeur M , Dierich A , Foidart JM . 1998 ; In vivo evidence that the stromelysin-3 metalloproteinase contributes in a paracrine manner to epithelial cell malignancy . *J Cell Biol* . 140 : 1535 - 41
- May P , Reddy YK , Herz J . 2002 ; Proteolytic processing of low density lipoprotein receptor-related protein mediates regulated release of its intracellular domain . *J Biol Chem* . 277 : 18736 - 43
- Metcalf P , Fusek M . 1993 ; Two crystal structures for cathepsin D: the lysosomal targeting signal and active site . *Embo J* . 12 : 1293 - 302
- Mohamed MM , Sloane BF . 2006 ; Cysteine cathepsins: multifunctional enzymes in cancer . *Nat Rev Cancer* . 6 : 764 - 75
- Montel V , Gaultier A , Lester RD , Campana WM , Gonias SL . 2007 ; The low-density lipoprotein receptor-related protein regulates cancer cell survival and metastasis development . *Cancer Res* . 67 : 9817 - 24
- Mueller MM , Fusenig NE . 2004 ; Friends or foes - bipolar effects of the tumour stroma in cancer . *Nat Rev Cancer* . 4 : 839 - 49
- Obermeyer K , Krueger S , Peters B , Falkenberg B , Roessner A , Rocken C . 2007 ; The expression of low density lipoprotein receptor-related protein in colorectal carcinoma . *Oncol Rep* . 17 : 361 - 7
- Rijnbouts S , Kal AJ , Geuze HJ , Aerts H , Strous GJ . 1991 ; Mannose 6- phosphate-independent targeting of cathepsin D to lysosomes in HepG2 cells . *J Biol Chem* . 266 : 23586 - 92
- Rochefort H , Liaudet-Coopman E . 1999 ; Cathepsin D in cancer metastasis: a protease and a ligand . *Apmis* . 107 : 86 - 95
- Rodriguez J , Vazquez J , Corte MD , Lamelas M , Bongera M , Corte MG , Alvarez A , Allende M , Gonzalez L , Sanchez M . 2005 ; Clinical significance of cathepsin D concentration in tumor cytosol of primary breast cancer . *Int J Biol Markers* . 20 : 103 - 11
- Slentz-Kesler K , Moore JT , Lombard M , Zhang J , Hollingsworth R , Weiner MP . 2000 ; Identification of the human Mnk2 gene (MKNK2) through protein interaction with estrogen receptor beta . *Genomics* . 69 : 63 - 71
- Song H , Li Y , Lee J , Schwartz AL , Bu G . 2009 ; Low-density lipoprotein receptor-related protein 1 promotes cancer cell migration and invasion by inducing the expression of matrix metalloproteinases 2 and 9 . *Cancer Res* . 69 : 879 - 86
- Strickland DK , Ranganathan S . 2003 ; Diverse role of LDL receptor-related protein in the clearance of proteases and in signaling . *J Thromb Haemost* . 1 : 1663 - 70
- Vignon F , Capony F , Chambon M , Freiss G , Garcia M , Rochefort H . 1986 ; Autocrine growth stimulation of the MCF 7 breast cancer cells by the estrogen-regulated 52 K protein . *Endocrinology* . 118 : 1537 - 45
- von Arnim CA , Kinoshita A , Peltan ID , Tangredi MM , Herl L , Lee BM , Spoelgen R , Hshieh TT , Ranganathan S , Battey FD . 2005 ; The low density lipoprotein receptor-related protein (LRP) is a novel beta-secretase (BACE1) substrate . *J Biol Chem* . 280 : 17777 - 85
- Wu L , Gonias SL . 2005 ; The low-density lipoprotein receptor-related protein-1 associates transiently with lipid rafts . *J Cell Biochem* . 96 : 1021 - 33
- Yang M , Huang H , Li J , Li D , Wang H . 2004 ; Tyrosine phosphorylation of the LDL receptor-related protein (LRP) and activation of the ERK pathway are required for connective tissue growth factor to potentiate myofibroblast differentiation . *Faseb J* . 18 : 1920 - 1
- Zhang H , Links PH , Ngsee JK , Tran K , Cui Z , Ko KW , Yao Z . 2004 ; Localization of low density lipoprotein receptor-related protein 1 to caveolae in 3T3-L1 adipocytes in response to insulin treatment . *J Biol Chem* . 279 : 2221 - 30
- Zurhove K , Nakajima C , Herz J , Bock HH , May P . 2008 ; Gamma-secretase limits the inflammatory response through the processing of LRP1 . *Sci Signal* . 1 : ra15 -

Figure 1

Pro-cath-D secreted by cancer cells stimulates the 3D outgrowth of human mammary fibroblasts independently of its catalytic function

(A) Outgrowth of HMF fibroblasts co-cultured with MCF-7 breast cancer cells whose pro-cath-D secretion of which was inhibited by siRNA silencing. HMF fibroblasts were embedded in Matrigel with or without a bottom layer of MCF-7 cancer cells (panel a). Phase contrast optical photomicrographs of HMF fibroblasts embedded alone (panel b, right) or in the presence of a bottom layer of MCF-7 cells (panel b, left and middle) after 3 days of co-culture are shown. High magnifications of the boxed regions are displayed below. Phase contrast optical photomicrographs of MCF-7 cells transfected with cath-D or luc siRNAs after 3 days of co-culture are presented (panel c). Expression and secretion of pro-cath-D were monitored in MCF-7 cell lysates (C) and media (S) before the beginning of the co-culture, and then in the media at day 1 to 3 of co-culture by western blot (panel d). Secretion of pro-cath-D was also monitored in media of HMF cells embedded alone at day 3 of co-culture (panel d). Expression of cath-D in a HMF lysate (C) is shown. (B) Outgrowth of HMF fibroblasts co-cultured with 3Y1Ad12 cancer cells secreting no procath-D, pro-cath-D or ^{D231N} pro-cath-D. HMF fibroblasts were embedded with or without a bottom layer of 3Y1Ad12 cancer cell lines secreting no pro-cath-D (control), human wild-type (pro-cath-D), or D231N pro-cath-D (D231N) as described in Fig. 1A (panel a). Phase contrast optical photomicrographs of HMF fibroblasts after 3 days of co-culture are shown (panel a). High magnifications of the boxed regions are displayed below. Phase contrast optical photomicrographs of 3Y1-Ad12 cancer cell lines after 3 days of co-culture are presented (panel b). Pro-cath-D secretion was analyzed after 3 days of co-culture by western blot (panel c). Arrows indicate fibroblasts. Bars (---, 50 μ m). *, non-specific contaminant protein. K, molecular mass in kilodaltons.

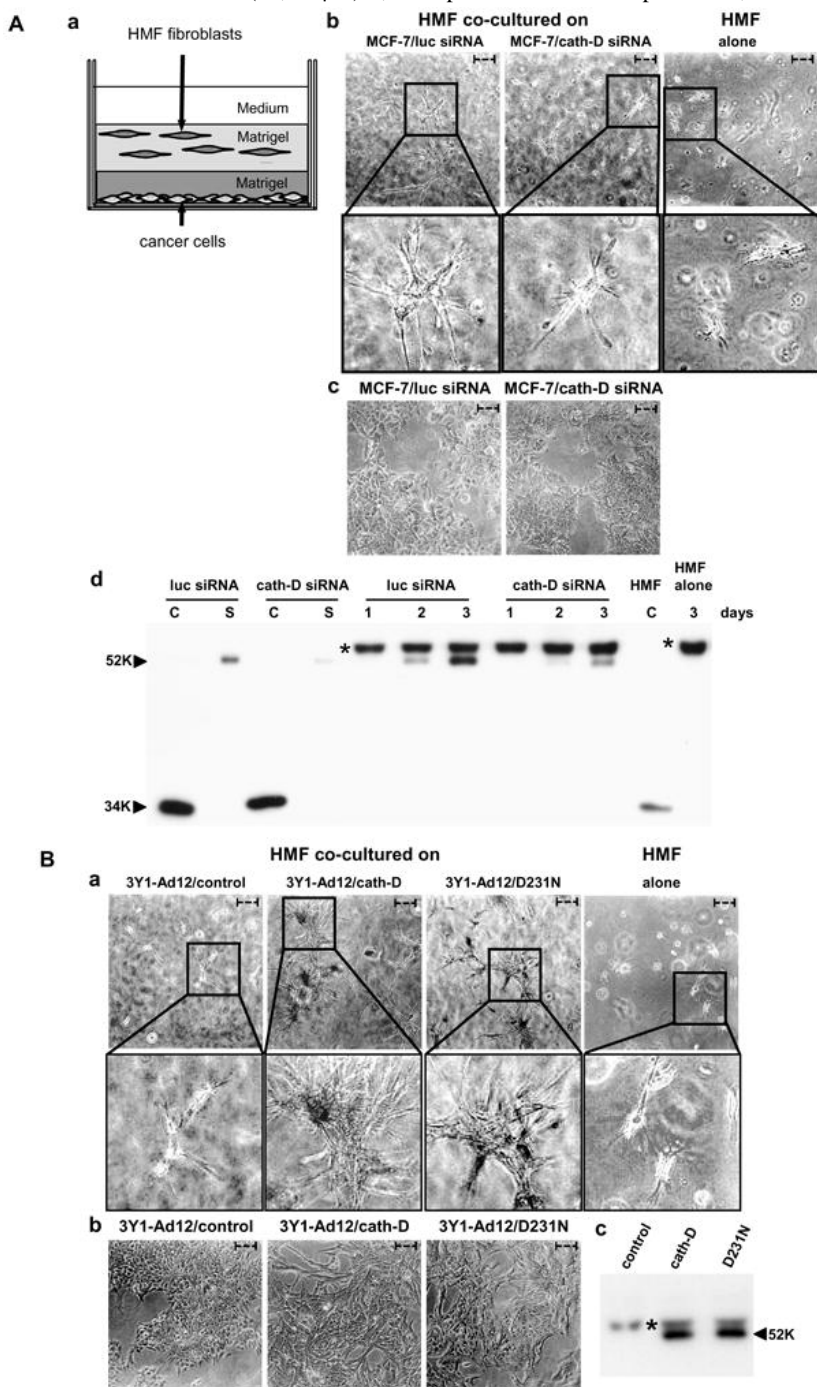


Figure 2Pro-cath-D interacts with the β chain of LRP1 in vitro

(A) Sequence of the LRP1 β chain interacting with cath-D isolated by yeast two-hybrid. LRP1 is synthesized as a 4544-amino acid precursor that is cleaved into an α chain and a β chain. The sequence of the β chain is shown, with the amino acids numbered starting at the first residue of the β chain. Residues 307-479, isolated by the yeast two-hybrid method, are shown in bold. The trans-membrane sequence is underlined, and the two Asn-Pro-X-Tyr (NP_XY) endocytosis motifs are in italics. **(B) Binding of pro-cath-D to LRP1 β (307-479) by GST pull-down.** Radio-labeled pre-pro-cath-D proform synthesized from the reticulocyte lysate system was incubated with glutathione-Sepharose beads containing GST-LRP1 β (307-479) or GST. GST proteins stained by Coomassie are shown in left panel. Bound pre-pro-cath-D was detected by autoradiography (right panel). **(C) Binding of the full-length extracellular domain of LRP1 β to pro-cath-D by GST pull-down.** The radio-labeled, full-length extracellular domain of LRP1 β (1-476) was incubated with beads containing GST-cath-D/52K, GST-cath-D/34K, GST-cath-D/14K, GST-cath-D/4K, or GST. GST proteins were stained by Coomassie (left panels). Bound LRP1 β (1-476) was detected by autoradiography (right panels). The input (1/10) corresponds to the lysate used for the binding reaction. K, molecular mass in kilodaltons.

A

1	QIDRGVTHLN	ISGLKMPRGI	AIDWVAGNVY	WTDGSRDVIE	VAQMKGENRK
51	TLISGMIDEP	HAIIVDPLRG	TMYSWSDWGNH	PKIETAAMDG	TLRETLVODN
101	IQWPTGLAVD	YHNERLYWAD	AKLSVIGSIR	LNQTDPIVAA	DSKRGLSHPF
151	SIDVFEDYIY	GVTYINNRVAF	KHKFGHSRL	VNLTGGLSHA	SDVLLYHQHK
201	QPEVYINPQDR	KKGEWLCLLS	PSGFVCTCPN	GKRLDKSTCV	PVSPPTPPD
251	APRPGTCLNQ	CFNGSGSFLN	ARRQPKRCRQ	PRYTGDKCEL	DOCWEHCRNG
301	GTCASPSGM	PTCRCPGTFT	GPKCTQQVCA	GYCANNSTCT	VNQGNGPQCR
351	CLPQFLG DRC	QYRQCSGYCE	NFGTCQMAAD	GSRCRCRTAY	FEGSRCEVNK
401	CSRLEGACV	VNKQSGDVTC	NCTDGRVAPB	CLTCVGHCSN	GGSCTMNSKM
451	MPECCQPPHM	TGPRCEEHVF	SQQQPHIAS	ILIPLLLLL	LVLVAGVVEW
501	YKRRVQGAAG	FQHORMTNGA	MNVEIGNPTY	KMYEGGE PDD	VGGLLDADFA
551	LDPDKPTNFT	NPVYATLYMG	GHGSRHSLAS	TDEKRELLGR	GPEDEIGDPL
601	A				

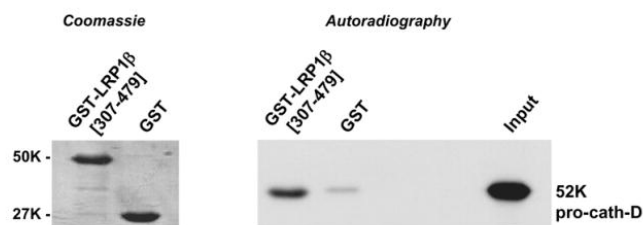
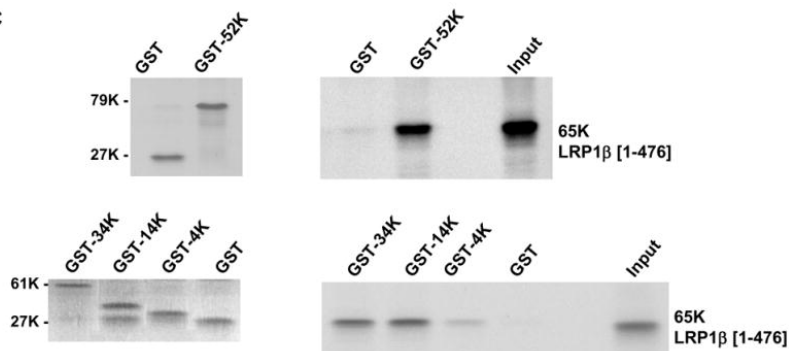
B**C**

Figure 3Pro-cath-D binds to residues (349-394) of LRP1 β in vitro

(A) Schematic representation of the LRP1 β extracellular domain and GST-LRP1 β fragments. A schematic representation of EGF-like repeats 16 to 22 located in the full-length extracellular domain of LRP1 β is shown in panel a. The F0 (307-479) fragment, which interacts with cath-D, is indicated by a dotted line. GST-LRP1 β fragments (F4, F6, F7 and F8) were derived from F0 (panel b). The F4 (349-394) GST-LRP1 β fragment was then sub-divided into 7 fragments (F5, F9-F14) (panel b). **(B) Binding of pro-cath-D to GST-LRP1 β fragments.** Radio-labeled pre-pro-cath-D was incubated with beads containing GST-LRP1 β fragments or GST. GST proteins bound to beads were stained by Coomassie (left panels a-c), and bound pre-pro-cath-D was detected by autoradiography (right panels a-c). The binding of pre-pro-cath-D to the fragments derived from F0 is shown in panel a. The binding of pre-pro-cath-D to fragments derived from F4 is shown in panel b. The binding of pre-pro-cath-D after GST-F0 and GST-F4 refolding is shown in panel c. The input (1/10) corresponds to the lysate used for the binding reaction. K, molecular mass in kilodaltons.

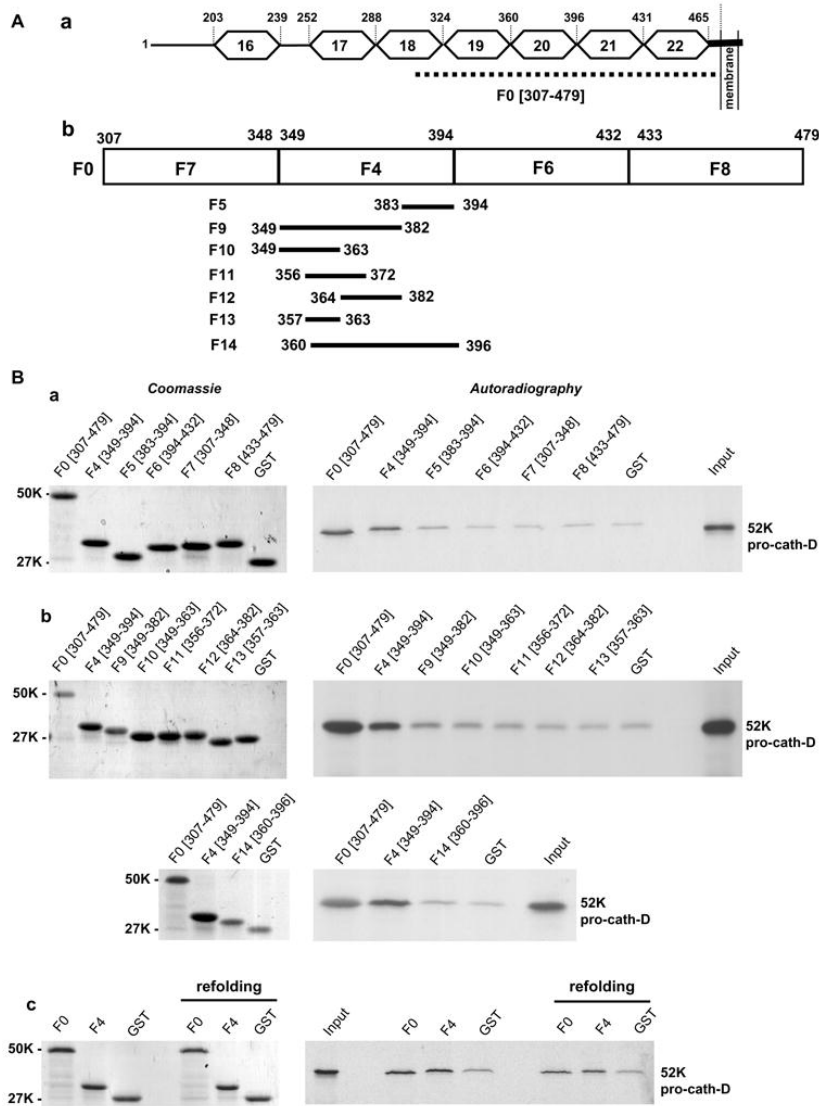
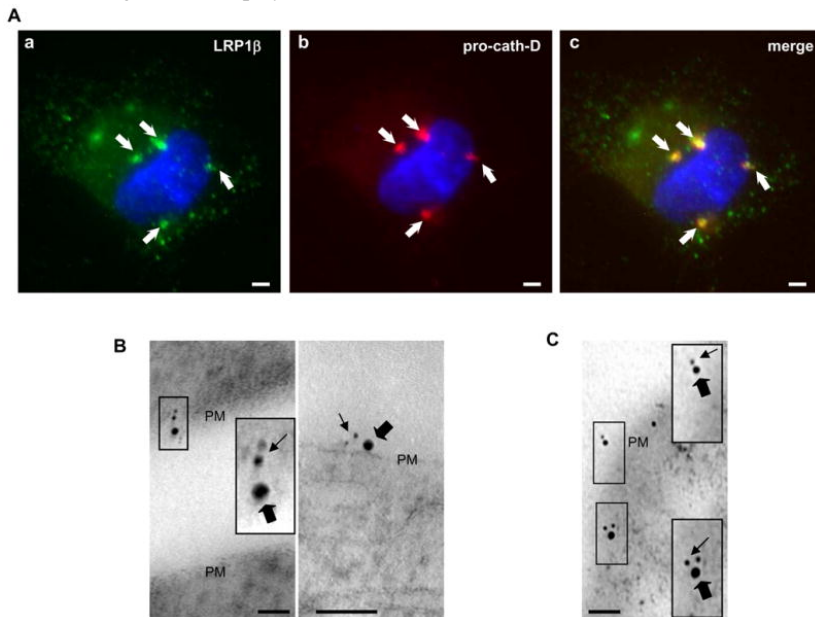


Figure 4

Pro-cath-D and LRP1 β partially co-localize at the cell surface in transfected COS cells and human mammary fibroblasts

(A) Co-transfected pro-cath-D and LRP1 β co-localize partially in punctuate structures. Non-permeabilized COS cells transiently co-expressing cath-D and Myc-LRP1 β were stained with a monoclonal anti-cath-D recognizing only the proform (red) and a polyclonal anti-Myc tagged LRP1 β (green) antibody. DNA was visualized by incubation with 0.5 μ g/ml cell-permeant Hoechst 33342 dye (blue). Panels a shows LRP1 β staining. Panel b shows pro-cath-D staining. Panel c shows the double-staining pattern. Arrows indicate pro-cath-D/LRP1 β co-localization. Bars, 15 μ m. **(B) Immunogold-labeled pro-cath-D and LRP1 β co-localize at cell surface in COS transfected cells.** COS cells transiently co-expressing cath-D and Myc-LRP1 β were double stained with a monoclonal anti-pro-cath-D antibody recognizing only the proform and conjugated to 6 nm gold particles (thin arrows), and with a polyclonal anti-LRP1 β antibody conjugated to 15-nm gold particles (thick arrows). Panels illustrate co-localization at the plasma membrane (PM). High magnifications of the boxed regions are displayed. Bars, 50 nm. **(C) Immunogold-labeled pro-cath-D and LRP1 β co-localize at the cell surface and in vesicular-like structures in human mammary fibroblasts.** COS cells were transfected with cath-D, and 48 h post-transfection conditioned medium containing 15 nM of pro-cath-D was added to HMF cells. HMFs incubated with pro-cath-D for 24 h were double stained with a monoclonal anti-pro-cath-D antibody recognizing only the proform and conjugated to 6-nm gold particles (thin arrows), and with a polyclonal anti-LRP1 β antibody conjugated with 15-nm gold particles (thick arrows). Panels illustrate co-localization at the plasma membrane (PM). High magnifications of the boxed regions are displayed. Bars, 50 nm.

**Figure 5**

LRP1 β enhances pro-cath-D localization in rafts in transfected COS cells

COS cells transfected with cath-D (panel a), or cath-D + LRP1 β (panel b) were unwashed and lysed 48 h post-transfection. Lysates were submitted to sucrose density ultracentrifugation. Fractions were analyzed for anti-LRP1 β (top panels) or anti-cath-D (middle panels) by immunoblotting. Cell lysates (100 μ g) from cath-D-transfected (CE1) and, cath-D + LRP1 β -co-transfected COS cells (CE2), were analyzed by immunoblotting. CE2 was loaded onto both gels (panels a and b) as an internal control for cath-D or LRP1 β enrichment relative to film exposure. Brackets indicate pro-cath-D and its neo-processed forms. Flotillin was used as a marker of raft fractions, and TfR as a marker of non-raft fractions (bottom panels). Each fraction was dot-blotted to detect ganglioside GM1 (bottom panels). K, molecular mass in kilodaltons.

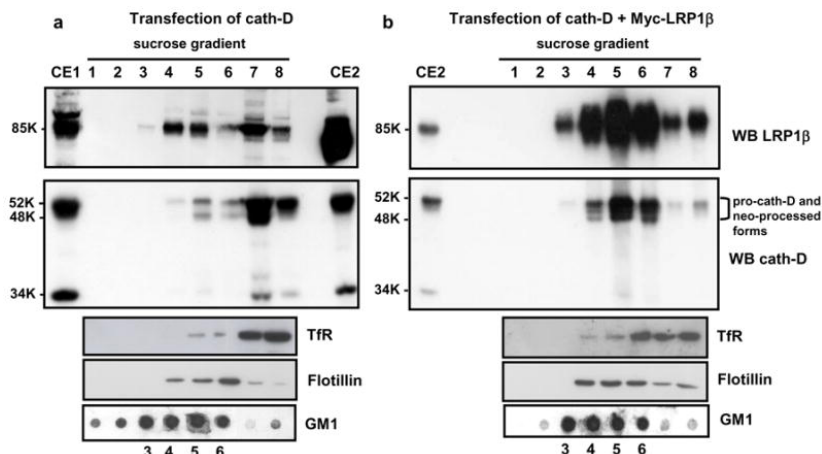


Figure 6Cath-D interacts with LRP1 β in transfected COS cells and in fibroblasts

(A) Co-immunoprecipitation of co-transfected pro-cath-D and LRP1 β in COS cells. COS cells were transiently co-transfected with LRP1 β expression vector, and pcDNA, cath-D, or D^{231N} cath-D vectors. 48 h post-transfection, unwashed cells were lysed in PLC buffer. Cell extracts (CE), and cath-D, LRP1 β and non-immune IgG immunoprecipitations (IP) performed with anti-LRP1 β 11H4 hybridoma or anti-cath-D MIG8 antibody were analyzed by anti-cath-D (panel a, top) and anti-LRP1 β (panel a, bottom) immunoblotting. Arrows show co-immunoprecipitated pro-cath-D. A longer gel exposure of the LRP1 β immunoprecipitation performed in COS cells co-transfected with LRP1 β and cath-D vectors and, analyzed by anti-cath-D immunoblotting is shown in panel b. **(B) Co-purification of endogenous LRP1 with cath-D in fibroblasts.** Co-purification of endogenous LRP1 with cath-D in cath-D-transfected MEFs (CD55^{-/-}-cath-D) (panel a). Cells grown to 90% confluence without medium change for 3 days were directly lysed in PLC buffer, and loaded on an anti-cath-D MIG8 affinity column that binds to 52-, 48-, and 34-kDa forms of cath-D. Eluted fractions were subjected to SDS-PAGE and immunoblotting with the anti-cath-D antibody (top panel) and anti-LRP1 β hybridoma (bottom panel). Co-purification of endogenous LRP1 with cath-D in HMF cells treated with pro-cath-D (panel b, left). COS cells were transfected with cath-D, and 48 h post-transfection conditioned medium containing 15 nM of pro-cath-D was added to HMF cells. Unwashed HMF fibroblasts incubated for 48 h with conditioned medium containing 15 nM of pro-cath-D were directly lysed in PLC buffer. HMF cell extracts were purified on the MIG8-coupled column and analyzed by immunoblotting as described in panel a. Detection of cath-D in a HMF lysate incubated with or without the conditioned medium containing pro-cath-D is shown in panel b (right). K, molecular mass in kilodaltons.

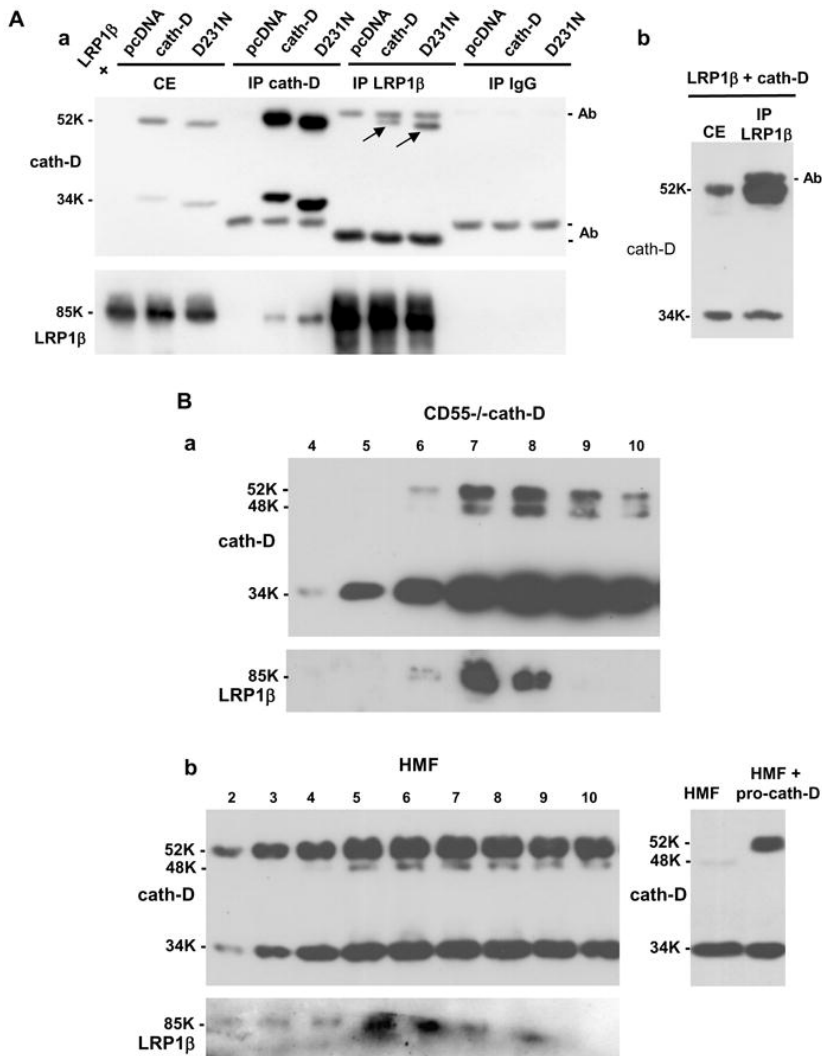


Figure 7

Silencing LRP1 inhibits the outgrowth capacities of cath-D and ^{D231N} cath-D secreting MEFs

(A) Matrigel outgrowth of cath-D transfected MEFs. CD55^{-/-}-SV40, CD55^{-/-}-cath-D, and CD55^{-/-}-D231N fibroblasts were embedded in Matrigel (panel a). Phase contrast optical photomicrographs of CD55^{-/-}-SV40, CD55^{-/-}-cath-D, and CD55^{-/-}-D231N fibroblasts are shown after culturing for 3 days (panel b). **(B) Silencing LRP1 in pro-cath-D secreting MEFs inhibits outgrowth.** CD55^{-/-}-cath-D cells transfected with LRP1 siRNA3 or Luc siRNA were embedded in Matrigel 24 h post-transfection (panel a). Phase-contrast optical photomicrographs (panel a, top), and p-nitrotetrazolium violet cell staining (panel a, bottom) are shown after culturing for 3 days. High magnifications of the boxed regions are displayed. For quantification, the number of outgrowth with protruding fibroblasts as detected with the p-nitrotetrazolium violet were counted by two independent investigators (double blind) in 3 low-magnification fields (panel b). *, p<0.0125; Student's t- test. LRP1 β expression was monitored 24 h post-transfection of CD55^{-/-}-cath-D cells with Luc siRNA or LRP1 siRNA3 (panel c). Bars: - - -, 75 μ m; -, 750 μ m. Data from one representative experiment out of 3 are shown. **(C) Silencing LRP1 in pro-^{D231N} cath-D secreting MEFs inhibits outgrowth.** CD55^{-/-}-D231N fibroblasts transfected with LRP1 siRNA3 or Luc siRNA were embedded in Matrigel 24 h post-transfection and analyzed as described in B. *, p<0.0125; Student's t- test.

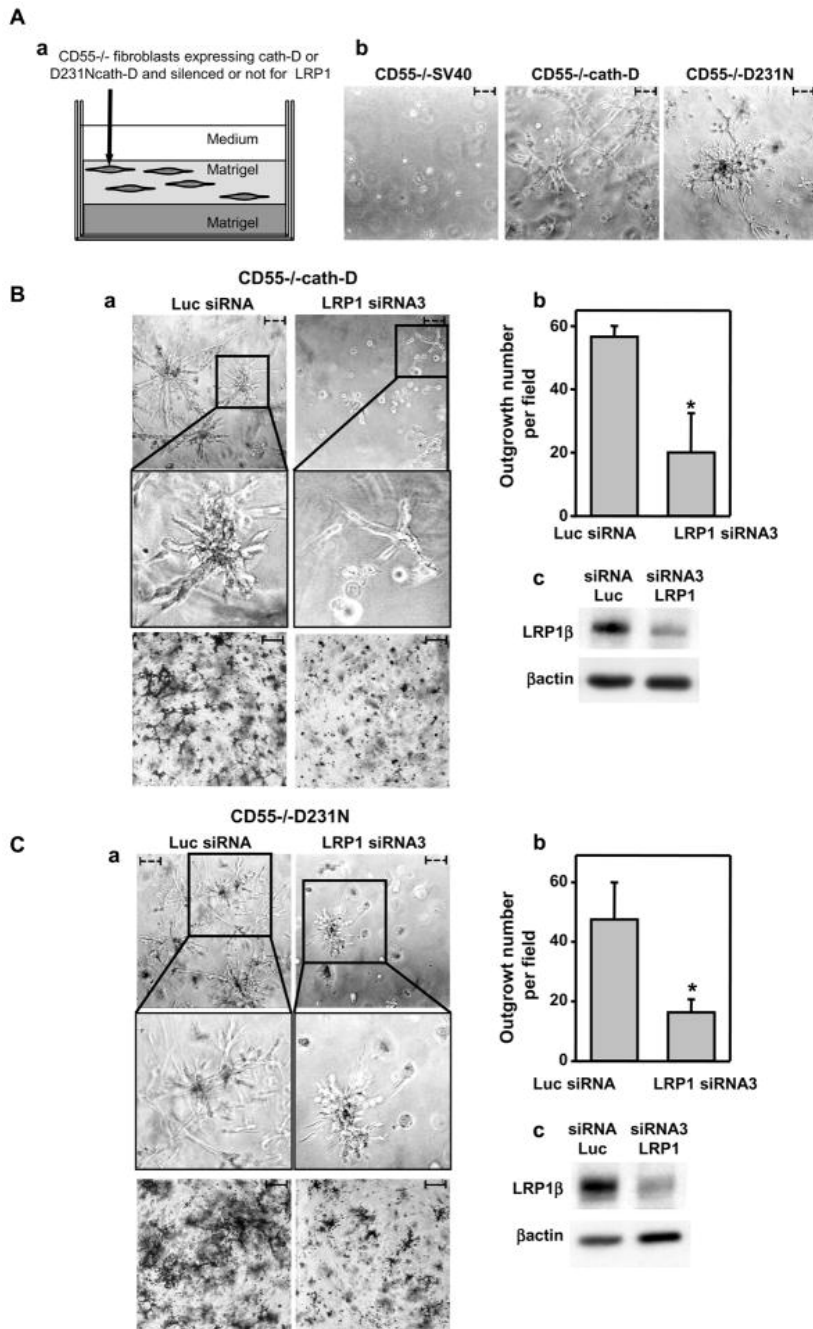


Figure 8

Silencing LRP1 in HMF fibroblasts inhibits the paracrine stimulation of fibroblast outgrowth induced by secreted pro-cath-D

HMFs transfected with Luc siRNA or LRP1 siRNA1 were embedded 48 h post-transfection in the presence of a bottom layer of 3Y1-Ad12 cancer cell lines secreting or not pro-cath-D or D231N pro-cath-D (panel a). LRP1 β expression was monitored 48 h post-transfection and before the co-culture assays (panel b). Pro-cath-D secretion was analyzed by immunoblotting after co-culturing for 3 days with Luc siRNA or LRP1 siRNA1 transfected HMFs, with 3Y1-Ad12 control or cath-D-transfected cells (panel c). Phase-contrast optical photomicrographs (panel d, top), and p-nitrotetrazolium violet cell staining (panel d, bottom) are shown after culturing for 3 days with HMFs transfected with Luc siRNA. Phase-contrast optical photomicrographs (panel e, top), and p-nitrotetrazolium violet cell staining (panel e, bottom) are shown after culturing for 3 days with HMFs transfected with LRP1 siRNA1. High magnifications of the boxed regions are displayed. Data from one representative experiment out of 3 is shown. *, non-specific contaminant protein. Bars; ---, 75 μ m; -, 750 μ m.

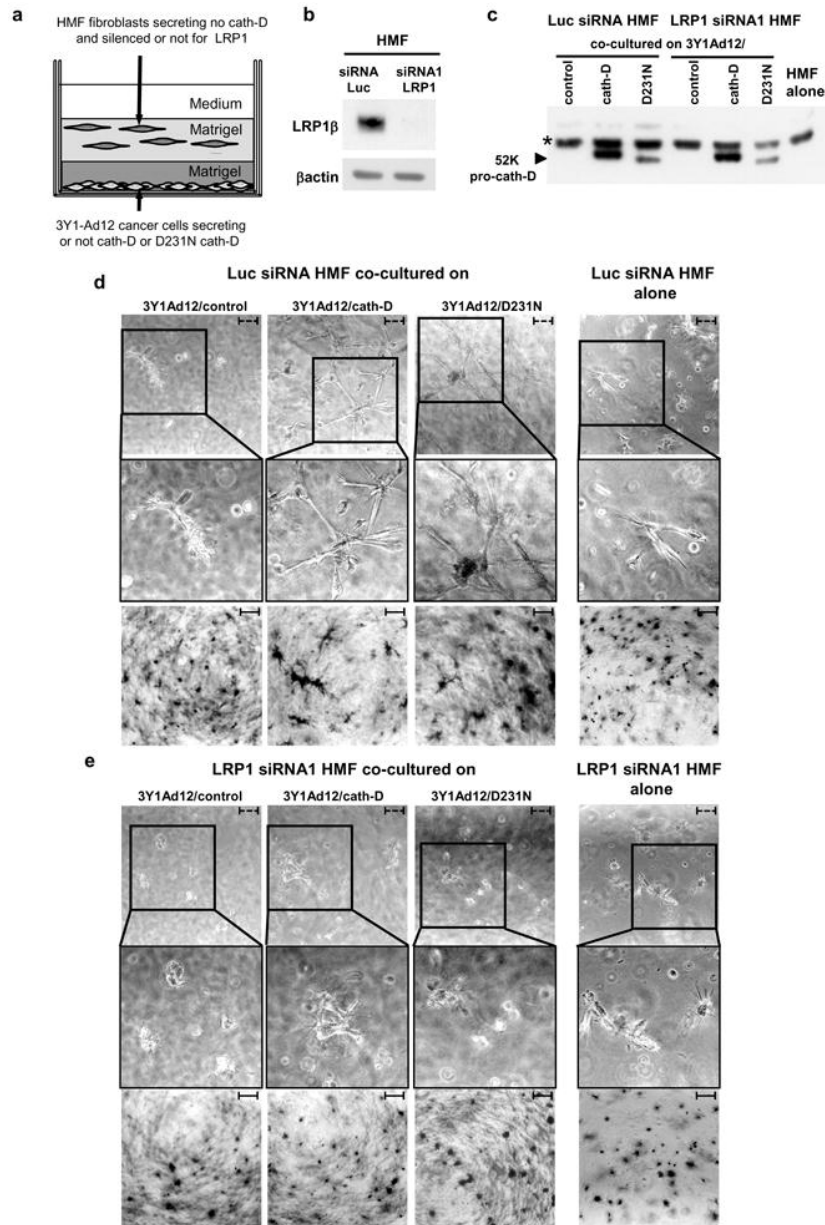


Figure 9

Model of cath-D paracrine action through the LRP1 receptor

We propose that pro-cath-D hypersecreted by cancer cells stimulates fibroblast outgrowth in a paracrine LRP1-dependent manner.

